Emission Spectrometry

DOI: 10.1002/anie.200802681

Atmospheric-Pressure Dielectric-Barrier Discharge as a Radiation Source for Optical Emission Spectrometry**

*Yongliang Yu, Zhuo Du, Mingli Chen, and Jianhua Wang**

Radiation sources employed for optical emission spectrometry include inductively coupled plasma,[1,2] microwave plasma,[3–5] laser-induced plasma,[6] and glow discharge.[7–9] The miniaturization of atomic spectrometric systems currently attracts much attention,[10] and studies have focused on the development of portable systems with high degrees of automation and robustness. A series of microradiation sources have been used for optical emission, for example, microfabricated inductively coupled plasma,[11] direct-current glow discharge,[12] solution-cathode glow discharge,[13] capacitively coupled microplasma,[14] and microwave microstrip plasma.[15,16] Dielectric-barrier discharge (DBD) generates low-temperature plasma at atmospheric pressure,[17,18] which is suitable for the atomization of volatile species.[19–21] It has also served as an ionization source for mass spectrometry[22,23] and ion mobility spectrometry.[24] In this respect, DBD provides a new approach for exploiting miniaturized atomic spectrometric systems.

In this work, an atmospheric-pressure DBD microplasma was used for the first time as a radiation source for a miniaturized optical emission spectrometric system. The portable system consists of a sample introduction unit, a DBD chamber, and a charge-coupled device (CCD) spectrometer as detector (Figure 1).

Sample introduction was achieved with mercury cold vapor generation by a microsequential injection unit (FIAlab Instruments, USA), furnished with two syringe pumps of 2.5 mL and 1.0 mL and a six-port selection valve. Two quartz plates ($50\times15\times1.2\ mm^3$) and two glass plates ($50\times5\times1\ mm^3$) form a gas channel ($50\times5\times1\ mm^3$) that serves as a radiation source. Two pieces of aluminum foil ($5\times30\ mm^2$) were attached onto the outer surface of the quartz plates to serve as electrodes for igniting and maintaining DBD microplasma by a 35 kHz high-frequency discharge generated by an ENT-106B neon power supply (Guangzhou Xinxing Neon Light Supply, China) at input voltages of 55–75 V at 50 Hz. The aluminum foils were placed 5 mm away from the brim of the exit of the radiation source. Cold mercury vapor was excited in the DBD chamber, and the emission spectra were recorded by a QE65000 CCD spectrometer (Ocean Optics, USA), with a slit width of 200 μm and an integrated HC1–QE composite blaze with a grating of 300 lines, which gives a resolution of approximately 8 nm. An integration time of 50 ms, an average of three scans, and a boxcar width of one were set for the CCD to ensure a reasonable signal-to-noise ratio and a proper spectral resolution.

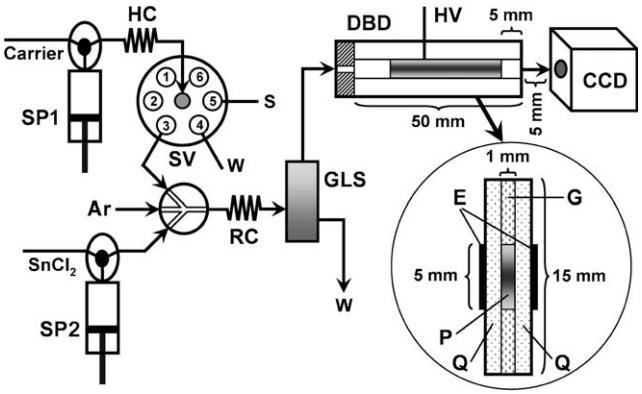

Figure 1. Schematic of the miniature DBD–OES system. SP1, SP2: syringe pumps; SV: six-port selection valve; HC: holding coil; RC: reaction coil; GLS: gas–liquid separator; HV: discharge power; E: discharge electrode; Q: quartz; G: glass; P: plasma; S: sample; W: waste. The inset illustrates the cross-sectional configuration of the DBD chamber.

The performance of the optical emission spectrometer is determined by the formation of microplasma and its excitation of mercury vapor, which is related to the discharge voltage and discharge electrode area. No plasma was obtained at a discharge voltage of less than 1.1 kV, whereas stable and homogeneous microplasma was observed at 1.20–1.80 kV. The power variations cause obvious changes in the optical emission of mercury recorded at 253 nm (Figure 2). A notable increase in emission was achieved by increasing the power from 1.20 to 1.35 kV, as higher voltage creates more high-energy electrons in the DBD which collide with argon and mercury vapor in the radiation source and thus promote the excitation of mercury and its subsequent emission. In subsequent experiments, a discharge power of 1.50 kV was employed. Moreover, a significant improvement in emission intensity was observed upon increasing the electrode area from 5×10 to $5\times30\ mm^2$ (Figure 2), attributed to the excitation of an increased number of mercury atoms. For the ensuing investigations, a discharge electrode area of $5\times30\ mm^2$ was used.

To examine the optical emission of mercury in the DBD radiation source, it is important to select an emission line with

[*] Dr. Y.-L. Yu, Z. Du, M.-L. Chen, Prof. J.-H. Wang
Research Center for Analytical Sciences, Box 332
Northeastern University
Shenyang 110004 (China)
Fax: (+86) 24-8367-6698
E-mail: jianhuajrz@mail.neu.edu.cn
Homepage: http://219.216.105.184/wjhktz/index.asp

[**] Financial support from the Natural Science Foundation of China (Key Project 20635010, National Science Fund for Distinguished Young Scholars 20725517, Major International Joint Research Project) and the 973 program (2007CB714503) are highly appreciated.

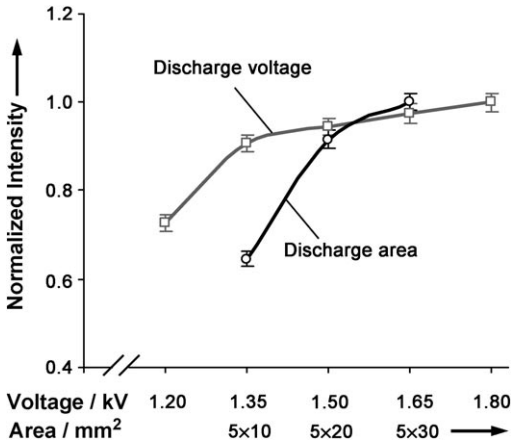

Figure 2. The dependence of mercury atomic optical emission at 253 nm on the discharge voltage and discharge electrode area. 500 μL of sample (10.0 μg L^{-1} Hg^{2+}) in HCl (1.0% *v*/*v*) and 400 μL of $SnCl_2$ solution (3.0% *m*/*v*) were used; sample loading time: 5 s.

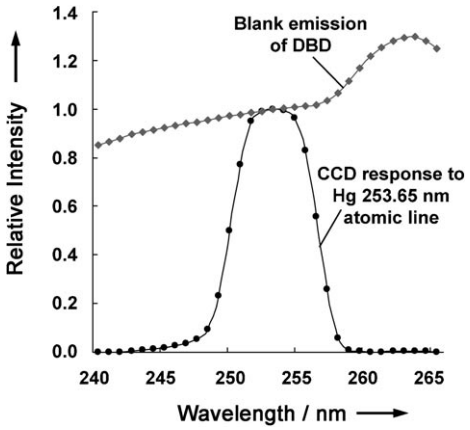

Figure 4. The CCD responses to blank emission of the DBD microplasma and the 253.65 nm mercury atomic line radiated from an HG-1 mercury argon calibration source.

favorable sensitivity while minimizing interfering effects. Thus, a blank emission spectrum of the argon DBD microplasma and one recorded in the presence of cold mercury vapor were studied (Figure 3). The emission line of mercury at 253.65 nm was clearly isolated from the blank emission spectra, and was adopted for quantification. The other strong atomic emission lines of mercury in the range of 296.73 nm to 435.84 nm were obscured by the blank emission, and the use of these lines for analysis is not feasible with the present system.

Figure 4 shows the responses of the CCD to blank emission of the DBD microplasma and the 253.65 nm mercury atomic line radiated from an HG-1 mercury argon calibration source (Ocean Optics, USA). The sharp radiation peak at 253.65 nm is observed as a relatively broad spectrum because of the insufficient resolution of the CCD. Nevertheless, a maximum intensity was recorded at 253 nm, and the CCD was set at this wavelength for further measurements.

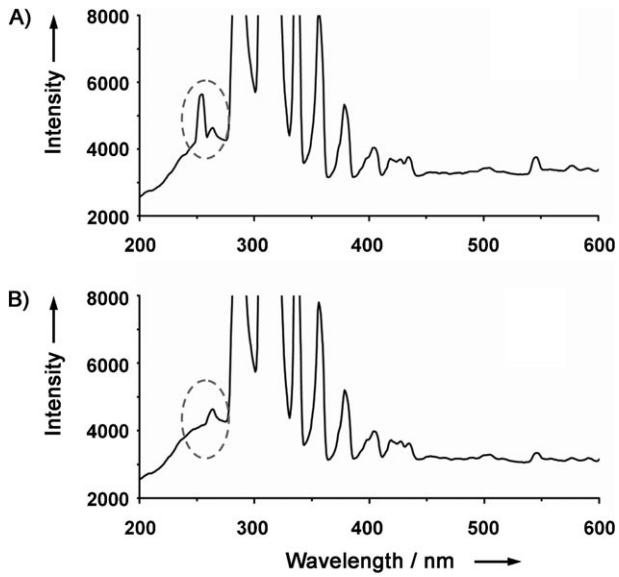

Figure 3. Optical emission spectra of the argon DBD microplasma recorded in the radiation source: A) in the presence of cold mercury vapor generated by 500 μL of sample solution (40 μg L^{-1} Hg^{2+}), showing clear isolation of the emission line at 253.65 nm from the blank spectra; B) blank emission spectra of the DBD microplasma.

The introduction of mercury vapor into the radiation source alters the microplasma, and the instability of the input and discharge power contributes an additional source of variation, resulting in large fluctuations in the emission of the DBD blank. This variation significantly deteriorates the accuracy, precision, and detection limit of the entire system. Investigations showed that fluctuations of blank emissions at two neighboring wavelengths (i.e., 245 nm and 253 nm) follow exactly a same trend; the emission at 245 nm is around 92% of that at 253 nm (Figure 4). Thus, a blank correction procedure was performed by first recording the optical emission simultaneously at 253 nm and 245 nm, and then a net emission spectrum at 253 nm was derived by subtracting the corresponding blank data at 245 nm. The CCD response at 245 nm for the 253 nm atomic line corresponds to less than 2% of the peak emission at 253 nm, which minimizes the error of the correction process. Figure 5 illustrates the significant improvement of the emission spectra after blank correction.

Cold mercury vapor generation is critical for its subsequent excitation and optical emission. Figure 6 shows the effects of argon flow rate, sample loading time, and concentration of $SnCl_2$ as reducing reagent. In our experiments, 1.0% *v*/*v* HCl was used for preparing the sample solutions and to generate the vapor, an argon flow rate of 100 mL min^{-1} was adopted, and a sample loading time of 5 s was employed for 500 μL of sample and 400 μL of $SnCl_2$ (3% *m*/*v*) solution.

The system tolerates a saline matrix of up to 5% *m*/*v* NaCl. No interference was found within a 5% error range for 5 mg L^{-1} of Cd^{2+}, Fe^{3+}, Cu^{2+}, Zn^{2+}, Cr^{3+}, Ni^{2+}, Pb^{2+}, Sb^{3+}, AsO_2^-, and SeO_3^{2-}. A detection limit of 0.2 μg L^{-1} was derived, which is comparable to those obtained by some other OES systems (Table 1). The system also offers a favorable sampling frequency of 90 h^{-1} and a relative standard deviation (RSD) value of 2.1% at 10.0 μg L^{-1} Hg^{2+}. Figure 7 shows the

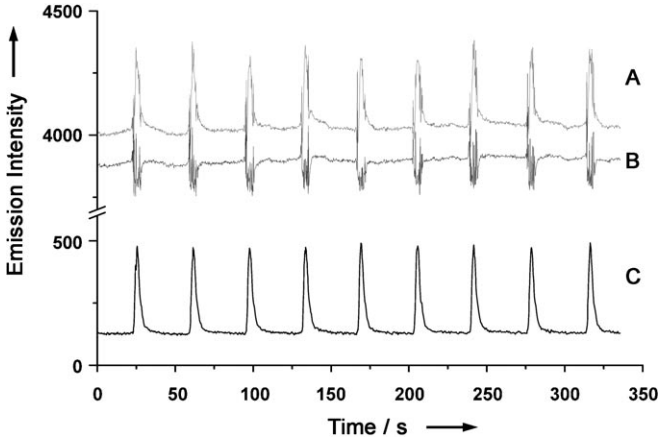

Figure 5. Blank correction for the emission spectra of mercury at 253 nm with respect to the blank emission of DBD microplasma obtained at 245 nm. A) The raw spectra recorded at 253 nm for 10 μg L^{-1} Hg^{2+}; B) the blank emission; C) the net emission spectra after performing blank correction.

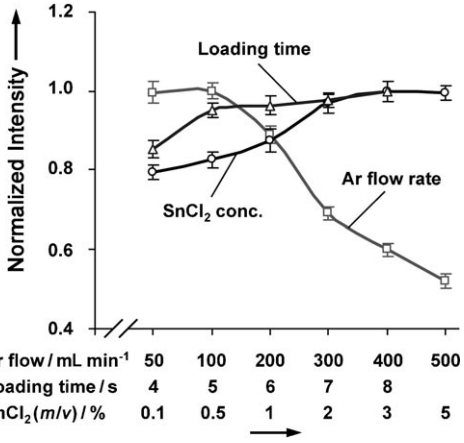

Figure 6. The dependence of mercury emission intensity on argon flow rate, sample/reagent loading time, and $SnCl_2$ concentration. 500 μL of sample solution (with 10.0 μg L^{-1} Hg^{2+}) in hydrochloric acid (1.0% *v*/*v*) was used; discharge voltage: 1.50 kV; discharge electrode area: 5×30 mm^2.

Table 1: Comparison of the detection limit (LOD) and precision (RSD) of the present system with those of other optical emission spectrometric systems for the determination of mercury.

Procedure	LOD [μg L^{-1}]	RSD [%]	Ref.
Inductively coupled plasma	0.21	1.7 (100)[a]	[1]
Solution-cathode glow discharge	22	1.9 (500)[a]	[13]
Microwave micro-strip plasma	0.11	5 (50)[a]	[15,16]
Radiofrequency glow discharge	0.2	4 (100)[a]	[25]
Radiofrequency discharge	0.1		[26]
Dielectric barrier discharge	0.2	2.1 (10)[a]	This method

[a] Concentration levels (μg L^{-1}) at which RSD values were obtained.

recorded spectral peaks and the calibration graph for 0.0–50.0 μg L^{-1} Hg^{2+} with a 500 μL sample solution.

The miniaturized portable optical emission spectrometric system was validated by analyzing mercury in certified

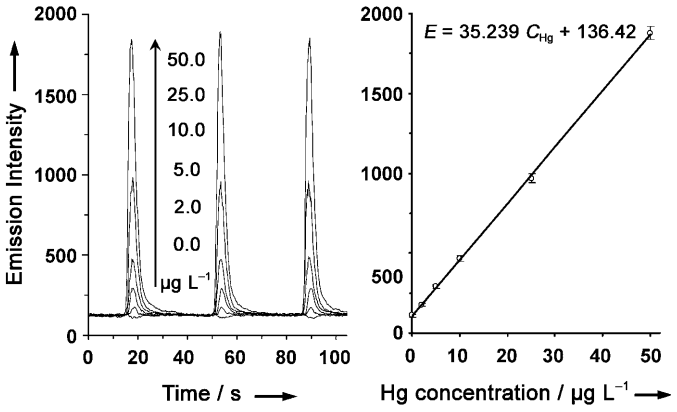

Figure 7. The recorded peak shapes and the calibration graph for 0.0–50.0 μg L^{-1} Hg^{2+}. 500 μL of sample solution in hydrochloric acid (1.0% *v*/*v*) and 400 μL of $SnCl_2$ solution (3.0% *m*/*v*) were used; discharge voltage: 1.50 kV; discharge electrode area: 5×30 mm^2; sample loading time: 5 s.

reference materials of CRM 176 (trace elements in a city waste incineration ash), NASS-5 (seawater), and SLRS-4 (riverine water). A reasonable agreement was achieved between the certified and the obtained values for CRM 176 (Table 2). As no mercury content was certified for NASS-5 and SLRS-4, the samples were spiked with mercury and satisfactory results were achieved.

Table 2: Determination of mercury in certified reference materials CRM 176, NASS-5, and SLRS-4 ($n=3$) by the present system.

Sample	Certified [μg g^{-1}]	Found [μg g^{-1}]	Spiked [μg L^{-1}]	Found [μg L^{-1}]	Recovered [%]
CRM 176	31.4±1.1	30.2±2.1			
NASS-5		n.d.[a]	10.0	9.9±0.4	99
SLRS-4		n.d.[a]	10.0	9.7±0.2	97

[a] n.d. = not detected.

Experimental Section

An argon stream at 100 mL min^{-1} was directed through the system prior to the operation. Meanwhile, the CCD was actuated to record the spectra. On changing samples, 200 μL sample solution was aspirated from port 5 and then dispensed through port 4 followed by 200 μL of carrier to clean the channels and eliminate residues from the previous sample. For each analysis, syringe pump SP1 was set to aspirate 500 μL of sample solution via port 5, while 400 μL of $SnCl_2$ solution was aspirated into SP2. Then, the sample solution followed by 500 μL carrier was successively dispensed by SP1 through port 3 at 12 mL min^{-1} to meet the $SnCl_2$ solution directed by SP2 at 4.8 mL min^{-1}. Upon confluencing, the reaction mixture was swept by an argon stream through the gas–liquid separator, where the cold mercury vapor was isolated and directed to the radiation source for optical emission and spectra recording.

Received: June 7, 2008
Revised: July 28, 2008
Published online: September 4, 2008

Keywords: cold microplasma · dielectric-barrier discharge · mercury · optical emission spectrometry

[1] M. Grotti, C. Lagomarsino, R. Frache, *J. Anal. At. Spectrom.* **2005**, *20*, 1365 – 1373.
[2] C.-Z. Huang, Z.-C. Jiang, B. Hu, *Talanta* **2007**, *73*, 274 – 281.
[3] H. Matusiewicz, M. Slachcinski, M. Hidalgo, A. Canals, *J. Anal. At. Spectrom.* **2007**, *22*, 1174 – 1178.
[4] B. Ozmen, F. M. Matysik, N. H. Bings, J. A. C. Broekaert, *Spectrochim. Acta Part B* **2004**, *59*, 941 – 950.
[5] M. Seelig, J. A. C. Broekaert, *Spectrochim. Acta Part B* **2001**, *56*, 1747 – 1760.
[6] C. Aragón, J. Bengoechea, J. A. Aguilera, *Spectrochim. Acta Part B* **2001**, *56*, 619 – 628.
[7] K. Wagatsuma, K. Kodama, H. Park, *Anal. Chim. Acta* **2004**, *502*, 257 – 263.
[8] B. Fernandez, N. Bordel, R. Pereiro, A. Sanz-Medel, *Anal. Chem.* **2004**, *76*, 1039 – 1044.
[9] A. Bengtson, C.-L. Yang, W. W. Harrison, *J. Anal. At. Spectrom.* **2000**, *15*, 1279 – 1284.
[10] R. Foest, M. Schmidt, K. Becker, *Int. J. Mass Spectrom.* **2006**, *248*, 87 – 102.
[11] O. B. Minayeva, J. A. Hopwood, *J. Anal. At. Spectrom.* **2003**, *18*, 856 – 863.
[12] J. C. T. Eijkel, H. Stoeri, A. Manz, *Anal. Chem.* **2000**, *72*, 2547 – 2552.
[13] M. R. Webb, F. J. Andrade, G. M. Hieftje, *Anal. Chem.* **2007**, *79*, 7899 – 7905.
[14] R. Guchardi, P. C. Hauser, *Analyst* **2004**, *129*, 347 – 351.
[15] P. Pohl, I. J. Zapata, E. Voges, N. H. Bings, J. A. C. Broekaert, *Microchim. Acta* **2008**, *161*, 175 – 184.
[16] I. Jiménez Zapata, P. Pohl, N. H. Bings, J. A. C. Broekaert, *Anal. Bioanal. Chem.* **2007**, *388*, 1615 – 1623.
[17] M. Miclea, K. Kunze, G. Musa, J. Franzke, K. Niemax, *Spectrochim. Acta Part B* **2001**, *56*, 37 – 43.
[18] H. R. Snyder, G. K. Anderson, *IEEE Trans. Plasma Sci.* **1998**, *26*, 1695 – 1699.
[19] Z.-L. Zhu, S.-C. Zhang, Y. Lv, X.-R. Zhang, *Anal. Chem.* **2006**, *78*, 865 – 872.
[20] Y.-L. Yu, Z. Du, M.-L. Chen, J.-H. Wang, *J. Anal. At. Spectrom.* **2008**, *23*, 493 – 499.
[21] Z.-L. Zhu, J.-X. Liu, S.-C. Zhang, X. Na, X.-R. Zhang, *Spectrochim. Acta Part B* **2008**, *63*, 431 – 436.
[22] N. Na, M.-X. Zhao, S.-C. Zhang, C.-D. Yang, X.-R. Zhang, *J. Am. Soc. Mass Spectrom.* **2007**, *18*, 1859 – 1862.
[23] N. Na, C. Zhang, M.-X. Zhao, S.-C. Zhang, C.-D. Yang, X. Fang, X.-R. Zhang, *J. Mass Spectrom.* **2007**, *42*, 1079 – 1085.
[24] A. Michels, S. Tombrink, W. Vautz, M. Miclea, J. Franzke, *Spectrochim. Acta Part B* **2007**, *62*, 1208 – 1215.
[25] R. Martínez, R. Pereiro, A. Sanz-Medel, N. Bordel, *Fresenius J. Anal. Chem.* **2001**, *371*, 746 – 752.
[26] R. Uhl, O. Wolff, J. Franzke, U. Haas, *Fresenius J. Anal. Chem.* **2000**, *366*, 156 – 158.

